Plasma deposition of piezoelectric ZnO layers by rf sputtering, SolGel and pulsed laser deposition

Kerstin Wätje, Jens Ebbecke, Götz Thorwarth, Mark van de Ven, Achim Wixforth

Angaben zur Veröffentlichung / Publication details:

Wätje, Kerstin, Jens Ebbecke, Götz Thorwarth, Mark van de Ven, and Achim Wixforth. 2008. "Plasma deposition of piezoelectric ZnO layers by rf sputtering, SolGel and pulsed laser deposition." *physica status solidi (c)* 5 (4): 943–46. https://doi.org/10.1002/pssc.200778334.

Plasma deposition of piezoelectric ZnO layers by rf sputtering, SolGel and pulsed laser deposition

Kerstin Wätje[1,*], Jens Ebbecke[1], Götz Thorwarth[2], Mark van de Ven[2], and Achim Wixforth[1]

[1] Institut für Physik der Universität Augsburg, Experimentalphysik I, Universitätsstraße 1, 86135 Augsburg, Germany
[2] Institut für Physik der Universität Augsburg, Experimentalphysik IV, Universitätsstraße 1, 86135 Augsburg, Germany

[*] Corresponding author: e-mail kerstin.waetje@physik.uni-augsburg.de, Phone: +49-821-598 3308, Fax: +49-821-598 3225

As „lab-on-a-chip-devices" suited for analyses of least amounts of liquids are emerging from prototype status, cost-effective materials for mass production of these devices are sought. For handling and mixing components, surface acoustic waves generated by piezoelectric elements are routinely employed; however, the $LiNbO_3$ single crystals used in such units are a significant cost factor. As an alternative, zinc oxide layers deposited onto the glass substrates hold the promise of cheaper production and easier integration into the assembly. In the present study, experiments regarding the deposition of such layers using different plasma processes are presented. Film synthesis was performed using rf magnetron sputtering, pulsed laser deposition and plasma based ion bombardment of Sol-Gel films on crystalline and amorphous substrates. The impacts of significant deposition parameters are discussed. At optimum deposition parameters, excellent columnar growth in the preferred c-axis orientation could be observed. The suitability of such films for the desired application is substanciated through first mixing experiments using optically lithographed interdigital transducers (IDTs).

1 Introduction ZnO is presently an attractive material due to three key properties. These are semiconductivity with a direct wide band gap of 3.37 eV and a large excitation binding energy of 60 meV, biocompatibility and piezoelectricity [1]. An ordered c-axis orientation of ZnO crystallites perpendicular to the substrate surface is desirable for applications where crystallographic anisotropy is a prerequisite, e.g. piezoelectric surface acoustic waves (SAW) or acousto-optic devices. SAW induced acoustic streaming for the agitation and actuation of smallest amounts of fluids has recently attracted growing attention in the field of microfluidics since it enables new applications like "lab on a chip devices" [2, 3]. These miniaturized "micro-labs" hold the promise of cheaper and faster biological analysis even in cases were only small amounts of liquids are available. Due to the considerable prospects of microfluidic applications, cheaper alternatives apart from piezoelectric single crystal substrates like the conventionally used $LiNbO_3$ have to be considered. High performance piezoelectric ZnO films hold promise for that purpose and can be produced by different plasma deposition methods. Usually ZnO films are deposited by molecular beam epitaxy [4], chemical va-pour deposition [5], pulsed laser deposition [6] or sputtering [7]. A much cheaper method to prepare thin ZnO films on different host substrates is the Sol-gel process, since it is possible to produce cheap large area coatings. In this study, we describe a Sol-gel method combined with Plasma Based Ion Implantation (PBII) for preparation of crystalline ZnO and compare the suitability of such Sol-gel derived ZnO films with pulsed laser deposited and rf magnetron sputtered ZnO films

2 Experimental Zinc acetate was first dissolved in methanol and stirred for 5 minutes at 50 °C. Then, a suit-

able amount of methoxyethylamine (MEA) was added as a stabilisator. After stirring the solution for 0.5 hours at room temperature a homogenous and transparent solution was obtained. After a resting period of 24 hours the resulting concentrations of the solutions varied between 0.6 and 1.6 Zn^+ molar. The substrates were cleaned with acetone and isopropanol in ultrasonic. Films were dipped onto (100) silicon substrates and amorphous glass slides and dried at 60 °C for 1 hour. The withdrawal speed varied from 1.5 to 3.5 mm s^{-1}. Films were dipped up to three times until the desired film thickness was achieved. Afterwards the films were annealed at 150 °C to 1000 °C for 3 hours in air, to exhale redundant carbon, oxygen and hydrogen from the dipped layer. Ion implantation using Ar^{++}, H^+ and O^{++} followed using a conventional beamline in order to study the effects of ion impingement on layer thicknesses sufficient for analysis.

For comparison, thin ZnO films were also prepared using a radio frequency sputtering system and pulsed laser deposition. The base pressure of the sputtering system was in the range of 10^{-6} mbar and the process took place at a working pressure from 10^{-3} to 10^{-2} mbar in Ar atmosphere. The distance between substrate and ZnO target was 8 cm; rf power varied between 60 and 300 W. The gas flow was varied from 2 to 32 sccm Argon while pressure was kept constant. The deposition took place without a heater. Films were deposited on (100) silicon and amorphous glass slides. The pulsed laser deposition of ZnO was processed in a high vacuum system using a KrF excimer laser (LPX 305i / Lambda Physik) with pulse duration of 25 ns, a repetition rate of 8 Hz and a pulse energy of 575 mJ. The deposition was performed at a base pressure of $6.0 \cdot 10^{-5}$ mbar and a residual gas pressure during deposition of 0.1 mbar in O_2 atmosphere. The substrate temperature was varied between 450 °C and 750 °C. Films were ablated on (100) silicon and c-plane sapphire.

All films were characterized by Rutherford backscattering spectroscopy (RBS), elastic recoil detection analysis (ERDA) and energy dispersive X-ray analysis (EDX) to determine the composition of the layers. Structural examinations were performed by X-ray diffraction (XRD), scanning electron microscop (SEM) and transmission electron microscopy (TEM). The film thickness was measured using a surface profilometry system (DekTak 8).

3 Results and discussion

3.1 SolGel dipped ZnO films ZnO Sol-gel films were dip coated from different Sol concentrations. Good reproducibility of films was found for a sol concentration of 1.5 molar Zn^+ solution. Final thickness of about 121, 180 and 259 nm was obtained for the crystallized films deposited at 1.5, 2.5 and 3.5 mms^{-1}, respectively. RBS, ERDA and EDX analysis showed suitable compositions of the ZnO layers after annealing at $\geq$ 500 °C, so an annealing temperature of 600 °C was selected for further investigations. In a next step, different ions were implanted with different energies into the 600 °C annealed layers.

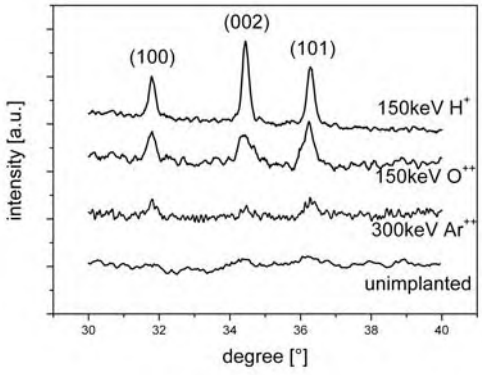

Figure 1 Diffraction pattern of SolGel dipped ZnO films annealed at 600 °C and implanted by different ions.

X-ray scans (Fig. 1) in Theta-2Theta-Geometry were performed to elucidate the influence of different ion species implanted in Sol-gel layers using a conventional implanter. It can be clearly seen that hydrogen implantation leads to the highest crystalline quality of the ZnO layers. The unimplanted films exhibit no diffraction peaks. As can be recognized in SEM pictures (see Fig. 2) only nanocrystals occur, whose XRD-signal cannot be seen in the diffraction pattern. By implanting ions in Sol-gel dipped films, energy input in collision cascades takes place which can lead to a coalescence of nano crystals. Heavier ions possess higher electronic and nuclear stopping power and so higher energy densities occur. This leads to a higher incorporation of defects and an amorphisation of ZnO films. As expected, argon implanted films show only rudimental diffraction peaks. ZnO layers implanted with oxygen ions exhibit low diffraction peaks and H^+ implanted ZnO films show clear (100), (101) and (002) diffraction peaks, were c-axis orientation seems to be more preferred for lighter ions. In further investigations H^+ ions were implanted into 600 °C annealed ZnO films by plasma based ion implantation (PBII) and conventional ion beamline. Hydrogen was selected as ion species because of its comparatively low nuclear energy loss, which limits amorphisation, and its high ion range at PBII voltages, which enables processing of thicker layers. In Fig. 2 three different SEM pictures are shown. The left picture displays an unimplanted ZnO layer with nanocrystallites. H^+ implantation by beamline leads to a coalescence of nanocrystals (middle picture). ZnO films handled with hydrogen PBII from an argon/hydrogen plasma, in contrast, exhibit larger crystals (right picture). However, because of chemical plasma etching in PBII a large part of the ZnO layer is desorbed and so no further film analysis were possible due to the marginal film thick-

ness. Further studies are necessary to limit this effect e.g. by PBII through a metallic grid.

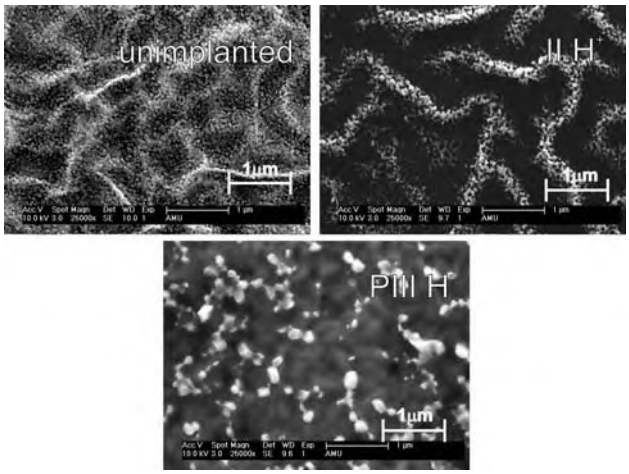

Figure 2 SEM pictures of an unimplanted ZnO layer (top left), a H^+ ion beam implanted layer (top right) and a H^+ plasma based ion implanted layer (bottom).

3.2 ZnO films grown with rf magnetron sputtering ZnO films deposited by rf magnetron sputtering from a pure ZnO target showed excellent stoichiometric qualities with almost no dependence on the sputtering parameters. Structural examinations, however, show a strong dependence on the rf power. Good c-axis orientation, which is necessary for piezoelectric applications, arises with higher rf power because of the occurrence of higher energetic particles in the plasma. Films deposited at 300 W exhibit a maximum relative intensity of the (002) peak and thus are expected to exhibit improved piezoelectric properties. The correlation of sputter parameters, film growth and structural properties can be understood in terms of the Thorthon model [8, 9], which describes the growth of sputtered materials in dependence of sputter pressure and substrate temperature. The general statement of this model is that increasing the substrate temperature and decreasing the sputter pressure leads to a more compact and dense film. In our case, the substrate temperature was kept at room temperature, while the correlation of sputter pressure and film quality was subject to further investigation (see Fig. 3).

For these studies, the ZnO films were deposited on amorphous glass slides (left panel) and (100) silicon (right panel) with different gas flow settings, keeping the deposition pressure constant. A higher gas-flow demands a faster pump down and thus contamination decreases. Rf power was kept constant at 300 W and deposition pressure at 1.0×10^{-2} mbar. The thicknesses of all layers were 1.5 µm to rule out the influence of layer thickness. A gas flow of about 20 sccm Argon resulted in a maximum relative intensity of the preferred c-axis peak. Higher gas flow cause smaller intensities as exposure time of the sputtergas declines. ZnO layers deposited on silicon show a shift of the

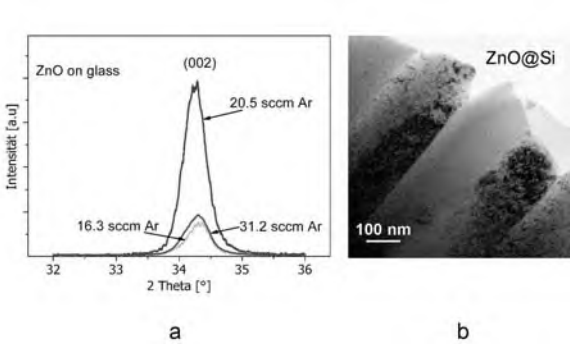

Figure 3 XRD pattern of sputtered ZnO films on glass slides with different gas flow (a); cross section TEM image of a sputtered ZnO layer on Si (b).

(002) peak with increasing peak intensity. Because of the lattice mismatch between silicon (100) and ZnO (002) a high intrinsic stress occurs in well orientated ZnO layers. This stress leads to a deviation of the position of the ZnO (002) diffraction peak and therefore is also an indication for high crystalline quality. ZnO layers deposited on amorphous glass slides stay unaffected of a lattice mismatch and exhibit no deviation. In the right picture a cross section TEM image of a sputtered ZnO layer on silicon is displayed. A columnar growth of ZnO is obtained with crystallite sizes of about 200 nm width. These results are in good agreement with X-ray and SEM measurements.

3.3 ZnO films deposited by PLD As a third method, ZnO films were also deposited on (100) silicon and c - plane Al_2O_3 as a substrate material by pulsed laser deposition. Depending on the residual O_2 pressure and substrate temperature during deposition, ZnO films grow with different crystalline qualities. To attain stoichiometric ZnO a residual O_2 pressure of at least 0.1 mbar was found to be necessary. Higher substrate temperatures cause a higher crystalline quality. These results are in good agreement with [10].

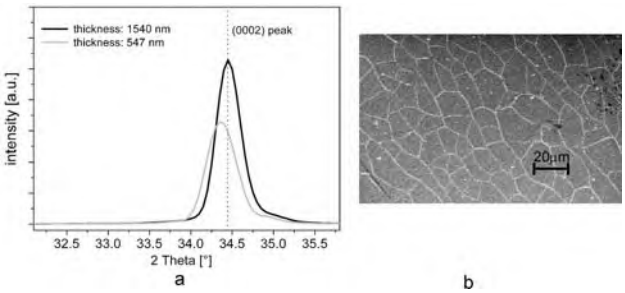

Figure 4 (a) XRD pattern of two ZnO layers produced on Si (100) by PLD with different thickness. The XRD peak of the thinner film is shifted left because of high stress. XRD peak of the thick layer is relaxed, because of a break up of the layer (b) SEM pictures of the thick sallied ZnO layer.

ZnO layers were deposited at a substrate temperature of 600 °C. Layers grown on sapphire exhibit less stress than those deposited on silicon, which might be due the greater difference in ZnO/Si thermal expansion coefficients compared to ZnO/Al_2O_3 [11,12]. The result was an increased cracking of layers deposited on silicon. In Fig. 4 (a) XRD pattern of two ZnO layers produced under the same process conditiones are shown. The thin layer exhibits a high stress and hence a shift of the XRD peak occures. The thick layer broke open during deposition and a relaxation of the layer took place. In the right picture (Fig. 4 b) a SEM picture of the thick sallied ZnO film occures.

Therefore,ZnO layers produced under the described parameter sets seem less likely to be adaptable for the use as piezoelectric layers on silicon and glass.

4 Initial mixing experiments Surface acoustic waves can be excited most commonly using metallic interdigitated electrodes on top of a piezoelectric substrate. The application of a radio frequency signal to such an interdigitated transducer (IDT) leads to the excitation of a SAW with a wavelength defined by the geometry of the IDT. This small surface displacement can couple efficiently to the liquid on top of the surface and induce acoustic streaming. Typical displacement amplitudes of a SAW are in the nanometer regime, and can be externally controlled by adjusting the excitation signal. In Fig. 5 an IDT on top of a ZnO layer is shown together with the principle of SAW propagation. In the right part a mixing experiment is shown. Here, small fluorescently labelled beads have been added to the fluid to visualize the acoustically induced streaming.

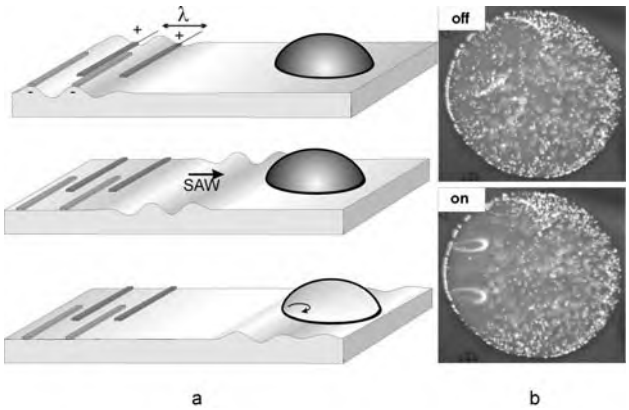

Figure 5 (a) Principle of a SAW propagation on a piezoelectric layer; (b) mixing of a droplet (1.0 mm diameter) on a sputtered piezoelectric ZnO layer. By applying an alternating voltage the droplet is stirred up.

5 Conclusion Different deposition methods for the formation of ZnO layers were examined. In matters of piezoelectric applications sputtered films showed excellent preferential c-axis orientation. ZnO films produced by PLD were not capable for these applications because of the high substrate temperature incurred and a breakup of the layers. The Sol-gel technique combined with PBII shows promising results, however further investigations are required. In first microfluidic experiments, the mixing of a small droplet on a sputtered ZnO layer was successfully operated.

Acknowledgements The author gratefully thanks the Bayrische Forschungsstiftung (ForOxid) for financial support. Financial support of the German Excellence Initiative via the "Nanosystems Initiative Munich (NIM)" is also gratefully acknowledged.

References

[1] Ü. Ötzgür, Y. Alivov, C. Liu, A. Teke et al., J. Appl. Phys. **98**, 41301 (2005).
[2] A. Wixforth, Physik in unserer Zeit **30**(3), 123 (1999).
[3] A. Wixforth, Superlattice Microstruct. **33**, 389 (2004).
[4] K. Iwata, P. Fons, S. Niki, A. Yamada, K. Matsubara, K. Nakahara, T. Tanabe, and H. Takasu, J. Cryst. Growth **214/215**, 50 (2000).
[5] T. Siosaki, S. Ohnishi, and A. Kawabata, J. Appl. Phys. **50**, 3113 (1979).
[6] S. Hayamizu, H. Tabata, H. Tanaka, and T. Kawai, J. Appl. Phys. **80**, 2 (1996).
[7] T. Yamamoto, T. Shiosaki, and A. Kawabata, J. Appl. Phys. **51**, 3113 (1980).
[8] J. A. Thornton, J. Vac. Sci. Technol. **11**, 666 (1974).
[9] J. A. Thornton, Ann. Rev. Mater. Sci. **7**, 239 (1977).
[10] M. Häberlen, Ionenstrahlsynthese und Charakterisierung großflächiger 3C-SiC-Pseudosubstrate für die Homo- und Heteroepitaxie, Dissertation, University of Augsburg, 2007.
[11] H. W. Lee, S. P. Lau, Y. G. Wang, B. K Tay, and H. H. Hng, Thin Solid Films **458**, 15 (2004)
[12] B. Kuhn, AlGaN/GaN-Heterostrukturen: Epitaxie und elektrische Eigenschaften, Dissertation, University of Stuttgart, 2002.